Applied Catalysis B: Environmental 180 (2016) 775–787

Contents lists available at ScienceDirect

Applied Catalysis B: Environmental

journal homepage: www.elsevier.com/locate/apcatb

The effect of iron loading and hydrothermal aging on one-pot synthesized Fe/SAPO-34 for ammonia SCR

Stanislava Andonova[a], Stefanie Tamm[a], Clifford Montreuil[b], Christine Lambert[b], Louise Olsson[a,*]

[a] Chemical Engineering, Chalmers University, 412 96 Gothenburg, Sweden
[b] Research and Innovation Center, Ford Motor Company, 2101 Village Road, Dearborn, MI, USA

ARTICLE INFO

Article history:
Received 1 May 2015
Received in revised form 30 June 2015
Accepted 7 July 2015
Available online 15 July 2015

Keywords:
NH_3 SCR
Fe/SAPO-34
Cu/CHA
One pot synthesis
Hydrothermal aging

ABSTRACT

The current commercially-available technique for NO_x reduction for diesel engines is the selective catalytic reduction (SCR) of NO_x with NH_3 over Cu zeolites. One of the problems of this technique is their limited ability to convert NO_x at diesel particulate filter (DPF) regeneration temperatures. In addition, during regeneration of the DPF there is a risk of thermally deactivating the SCR catalyst. Thus, the aim of the current work was the development of a catalytic system that can reduce NO_x both at low as well as high temperature and in addition is stable at high temperature. In order to reach this goal, a Fe/SAPO-34 with chabazite (CHA) structure was combined in a system with a commercial Cu/CHA catalyst. Earlier studies have shown that it is difficult to ion-exchange Fe into CHA structures due to steric hindrance, and we have therefore used a novel synthesis procedure which incorporated iron directly into the zeolite structure. Fe/SAPO-34 with three different Fe-loadings (0.27; 0.47 and 1.03 wt.% Fe) were synthesized and the catalysts were characterized using inductively coupled plasma atomic spectroscopy (ICP-AES), N_2 adsorption–desorption isotherms, BET area measurements and X-ray diffraction (XRD). The chemical composition, porous and crystalline structure of the parent SAPO-34 sample were found to be only slightly affected by addition of small amounts of Fe in the framework zeolite structure. However, more visible changes in the crystallinity were observed in the Fe/SAPO-34 catalysts with higher Fe content, which were attributed to the unit cell size expansion provoked by integration of higher amounts of Fe into the zeolite SAPO-34 framework. The Fe/SAPO-34 with the lowest Fe-loading (0.27 wt.%) was found to be the best catalyst when considering activity as well as high temperature stability. The synthesized Fe/SAPO-34 catalyst demonstrated a significantly improved NO_x reduction performance at high temperatures (600–750 °C) when compared to a commercial Cu/CHA SCR system, and the combined system (Fe/SAPO-34 + Cu/CHA) exhibited a very good performance in a large temperature interval (200–800 °C) that encompasses most diesel exhaust gas conditions.

1. Introduction

Increasing environmental concerns over the past several decades have resulted in the need to find innovative ways to deal with exhaust emissions produced by the lean combustion of fossil fuels. Achievement of high environmental standards for the emissions of nitrogen oxides (NO_x), unburned hydrocarbons and particulate matter (i.e., soot) from mobile and stationary sources remains an important challenge [1]. Thus, the need for better fuel economy, which diesel and lean burn gasoline engines possess, and more stringent NO_x emission standards have driven the development of different strategies of NO_x reduction in oxygen rich conditions [2,3]. One of the most effective NO_x abatement technologies is the selective catalytic reduction (SCR) of NO_x by NH_3, which is used for stationary power plants, industrial processes and also for automotives [2].

Many fundamental and more applied studies have been devoted to understand the basic mechanism of NH_3 SCR and to develop highly active and selective catalysts [4–6]. V_2O_5/WO_3 supported on anatase TiO_2 is one of the most commonly used and widely investigated SCR systems, for stationary applications [5,6]. In the last years, materials based on transition-metal ion-exchanged zeolites have received significant attention due to the improved NO_x reduction performance and thermal stability in a wide temperature range [2].

* Corresponding author. Fax: +46 31 772 3035.
E-mail address: louise.olsson@chalmers.se (L. Olsson).

http://dx.doi.org/10.1016/j.apcatb.2015.07.007
0926-3373/

Hence, different experimental and theoretical studies were focused on the effect of the metal (Cu, Fe, Ce, Co, and Ag) and type of the zeolites (ZSM-5, MFI, FER, BEA, SSZ-13, and SAPO-34) [4,7–9], on the stability and the overall SCR performance [7,9–12]. In general, Fe- and Cu- based zeolites are selected as the most active SCR catalysts for NO_x reduction [13,14]. In particular, it was found that the Cu-ion exchanged zeolites are characterized by superior low temperature activity [13,14]. On the other hand, Fe-based zeolites (mostly Fe/ZSM-5 and Fe/BEA) are known to be more active for SCR at higher temperatures (≥400 °C) [15–17]. Based on the effectiveness of the individual Fe/ZSM-5 and Cu/CHA based zeolites, recent studies showed that they could be combined in order to achieve high NO_x conversion over a broader temperature range [13,14].

However, there are several problems connected with using zeolites like ZSM-5 or BEA, like their relatively low hydrothermal stability, in combination with susceptibility towards hydrocarbon (HC) poisoning and coking [18–23]. This is the background for the development of a new class of hydrothermally stable small-pore zeolites, which have the chabazite (CHA) structure, and put into use on Ford U.S. diesel trucks in 2010 [24]. These Cu/CHA systems showed much better NO_x conversion efficiency and superior hydrothermal durability when compared to large (Cu/BEA or Cu/Y) or medium pore zeolites (Cu/ZSM-5) catalysts [10,12,25]. For example [26,27], silico-alumino-phosphate molecular sieves (SAPO) with chabazite related structures exhibited excellent stability of the framework at 1000–1200 °C. In addition the chabazite structure has a small pore radius (~3.8 Å), which hinders the hydrocarbons (HC) from entering the pores, resulting in a resistance to HC poisoning and coking [28]. Many efforts have been devoted in the last few years to the development of an NH_3-SCR catalyst based on Cu/SSZ-13 (SSZ-13 is the silico-aluminate form of the CHA structure) or Cu/SAPO-34 (silico-alumino-phosphate form of the CHA structure) [10,12,25,29,30].

One of the problems for the practical application of the current commercially available Cu/CHA catalysts for NH_3 SCR on diesel vehicles is their limited ability to convert NO_x at filter regeneration temperatures in excess of 450 °C [22]. A promising solution to this is to combine Fe/zeolite with Cu/zeolite [13,14]. However, the use of Fe/BEA and Fe/ZSM-5 gives problems with hydrothermal stability and HC tolerance. Therefore it would be a large advantage to combine Fe/CHA with Cu/CHA, but there are issues with preparing Fe/CHA.

The conventional wet ion exchange is one of the most commonly used methods for preparation of Fe/zeolite catalysts, replacing the H^+ or Na^+ cations of the zeolite structure by ferric ions [31,32]. However, this technique is challenging for the synthesis of Fe-containing SAPO-34 or other chabazite-like molecular sieves, because of the small pore size (~3.8 Å) of the zeolite matrices [28] and the larger ionic diameter [33] of the hydrated Fe^{3+} ions (9 Å). In a very recent work, an active Fe/SSZ-13 catalyst for NH_3 SCR was successfully synthesized by traditional aqueous solution ion-exchange method under the protection of N_2 [37]. The method used in the study was applied to prevent Fe^{2+} ions from being oxidized to bulky Fe^{3+} moieties (e.g., FeO(OH)) that can hardly penetrate into zeolite pores. It was demonstrated that the small pore CHA structure does not impede Fe^{2+} ion exchange and the formed Fe species become active at temperature above 400 °C after aging of the Fe/SSZ-13 catalyst. For potential practical applications, the authors suggested that Fe/SSZ-13 may be used as a co-catalyst together with Cu/CHA as integral after treatment SCR catalysts on the basis of the stable high temperature activity after hydrothermal aging [37]. Further, there exist a few studies in the literature addressing the hydrothermal synthesis of Fe/SAPO-34 catalysts, directly incorporating Fe into the structure, for the applications of chloromethane transformation to light olefins and of methanol conversion [34,35]. In a recent patent application, NH_3 SCR of Fe/SAPO-34, with Fe incorporated into the structure, was studied, but only up to 500 °C [36]. However, there are today no studies available that use one-pot synthesized Fe/SAPO-34 for NH_3 SCR in a broad temperature interval.

The objective of our work is therefore to use the novel synthesis method for incorporating the iron directly into the CHA structure during the zeolite synthesis. We have thereafter combined this Fe/SAPO-34 with Cu/CHA in a catalyst system and received high activity over a broad temperature interval (200–800 °C). A series of Fe/SAPO-34 catalysts with different Fe loadings (0.27, 0.47, and 1.03 wt.% Fe) were prepared by Fe incorporation directly in the SAPO-34 synthesis [38], adopted from the original method for pure SAPO-34 described by Prakash and Unnikrishnan [39]. Then, a combination of several characterization techniques was applied, such as inductively coupled plasma atomic spectroscopy (ICP-AES), N_2 adsorption–desorption isotherms, surface area measurements, and X-ray diffraction (XRD). In addition, to quantify the effect of the hydrothermal aging of the Fe/SAPO-34 and a commercial Cu/CHA SCR catalyst, multiple long-term and accelerated aging protocols were carried out by varying thermal treatment temperatures (800–900 °C) and time (1–80 h) of aging. For fresh and hydrothermally aged samples NH_3-storage/temperature-programmed desorption (TPD), 'standard' and 'rapid' NH_3 SCR were performed.

2. Experimental

2.1. Fe/SAPO-34 catalyst synthesis

The preparation of the Fe/SAPO-34 catalyst in the present study and in our patent application reported in Ref. [38] followed the procedure of hydrothermal synthesis in which the transition metal substituted SAPO material was prepared directly from a gel, adopted from the original method for synthesis of pure SAPO-34 described by Prakash and Unnikrishnan [39], with the following molar composition:

$$1.0Al_2O_3 : 1.06P_2O_5 : 1.08SiO_2 : xFe : 2.09\text{Morpholine} : 66H_2O$$

where x is the *mol* concentration of Fe, varied by changing the amount of Fe(III) nitrate nonahydrate precursor.

In a typical synthesis, the first step is to prepare a solution of ortho-phosphoric acid (H_3PO_4, 85 wt.%, *Merck)* dissolved in milli-Q water, which was stirred for 15 min at room temperature. Then, pseudoboehmite (74% Al_2O_3, PURAL SB-1, *Sasol*) was slowly added (within 2 h) to the diluted phosphoric acid solution. The slurry was stirred at room temperature for 12 h until a uniform gel was obtained. In the second step, iron(III) nitrate nonahydrate ($Fe(NO_3)_3{\cdot}9H_2O$, Sigma–Aldrich), separately dissolved in 10 ml H_2O, was dropwise added to the slurry (within 1 h) and stirred for 30 min. In the third step, a solution of colloidal silica (LUDOX AS-40, SiO_2, 40 wt.% in H_2O, *Aldrich*) and morpholine (tetrahydro-1,4-oxazine, *Sigma–Aldrich*) were separately prepared and after complete dissolution (within 10–15 min), the silica-morpholine containing mixture was under constant stirring slowly added (within 1 h) to the first alumina-P-Fe-containing solution at room temperature. Next, the slurry was continuously stirred for 7 h under ambient conditions. The obtained reaction mixture was aged at room temperature for 24 h without stirring. Then, the solution was transferred into a Teflon-lined stainless steel autoclave, sealed and heated for 72 h at 200 °C. The crystallization process was carried out under autogenic pressure without stirring. The crystallization time was recorded from the start of heating of the autoclave in the oven, which was pre-heated to 200 °C. After cooling to room temperature, the liquid phase was separated from the solid phase and the crystalline product was centrifuged, thoroughly washed with distilled water and dried at 100 °C for 12 h. Finally, the result-

ing product was ground into a fine powder form and calcined at 560 °C for 6 h using a ramp rate of 5 °C min^{-1}. The Fe/SAPO-34 catalysts with different Fe loadings were denoted as SF-1, SF-2 and SF-3, where SF-1 contains the smallest amount of iron and SF-3 the largest. For an accurate comparison, a pure SAPO-34 sample was prepared as reference material by using the procedure described above. In addition to this, pure commercial SAPO-34 (ACS Material, LLC) and commercial Cu/CHA (washcoated monoliths) catalysts were also used as reference materials.

2.2. Catalyst characterization techniques

The synthesized materials were characterized using several techniques. The elemental composition of the synthesized Fe/SAPO-34 catalyst was determined by an ICP-AES after $LiBO_2$-fusion and acid digestion of the samples. The textural properties of the samples previously degassed at 250 °C for 3 h were measured based on N_2 adsorption–desorption isotherms using a Micromeritics ASAP 2000 apparatus. BET surface area (S_{BET}) and total pore volume (V_{pores}) were calculated using the BET and Barrett–Joyner–Halenda (BJH) method, respectively. XRD patterns were recorded on a "Scintag X2" diffractometer equipped with a computer-controlled goniometer and an X-ray source with CoKα radiation (λ = 1.78897 Å). Diffraction patterns of the samples were recorded in 2θ range between 5 and 40° with step size/scan of 0.02° per second sampling interval.

2.3. Monolith washcoating

The calcined Fe/SAPO-34 powder was used to coat cordierite monoliths. The monoliths were cut from a commercial honeycomb cordierite structure (length = 20 mm, diameter = 22 mm and cell density of 400 cpsi) and heated to 500 °C for 2 h. A solid phase of 5 wt.% boehmite (Disperal D, Sasol, GmbH) dissolved in a liquid phase (distilled water/ethanol = 50/50) was first used for the impregnation of the calcined monoliths, in order to enhance the attachment of the SAPO-34. The alumina-coated monoliths were calcined at 500 °C for 2 h. Then the procedure consisted of immersing the monoliths into slurry composed of a liquid phase of equal amounts of distilled water and ethanol and a solid phase of 5 wt.% boehmite and 95 wt.% catalyst. The solid content in the slurry was 20% w/w. The procedure of the immersing, blowing away the excess slurry, drying (90 °C for 2 min) and heating (650 °C for 2 min) in air was repeated several times until the monolith was coated with the desired amount of washcoat (~700 mg), which corresponded to about 101 g L^{-1}. This low washcoat loading was chosen in order to minimize mass transport limitations. However, the activity would likely be even higher when using higher loadings. Finally, the washcoated monoliths were calcined at 500 °C for 2 h.

2.4. Hydrothermal aging of the catalysts

The hydrothermal treatment of the Fe/SAPO-34 and commercial Cu/CHA monolith samples was performed by using the experimental set-up which has been described in detail elsewhere [4,7]. Briefly, the monolith was inserted in the heated zone of a horizontal quartz tube reactor, which was equipped with an insulated heating wire controlled by a Eurotherm temperature-controller. The temperature was measured with a thermocouple positioned about 10 mm in front of the monolith and a second one placed in the center of the monolith. Water was introduced to the feed stream in the form of steam, via a controlled evaporation and mixing system from Bronkhorst. To simulate aging in lean hydrothermal conditions, the catalysts were exposed to a gas mixture consisting of 5% H_2O, 14% O_2, 5% CO_2, and Ar with a total gas flow of 3500 ml min^{-1}. Multiple long-term (at 800 °C for 80 h) and accelerated aging (at 800/850 °C for 24 h; at 900 °C for 1 h and 4 h) protocols were carried out.

2.5. Flow reactor measurements with monolith catalysts:

The reaction studies on the monolith catalysts were performed on the experimental set-up described above for the thermal aging experiments. The total gas flow was held constant at 3500 ml min^{-1}, yielding a space velocity of 30,300 h^{-1}, based on monolith volume. The monoliths were wrapped with quartz wool to ensure that no gas slipped around the sample. The outlet gas composition from the reactor flow was monitored and analyzed online with a MKS MultiGas 2030HS FTIR spectrometer. To maintain a constant catalytic behavior over the course of the study, the catalysts were initially degreened at 700 °C with 14% O_2 + 5% CO_2 + 5% H_2O in Ar for 5 min, followed by 350 ppm NO + 350 ppm NH_3 + 14% O_2 + 5% CO_2 + 5% H_2O in Ar for 30 min. Prior to each experiment, the catalysts were pre-treated at 700 °C in Ar using 14% O_2 + 5% CO_2 + 5% H_2O for 15 min. The following experiments were carried out:

2.5.1. NH_3 storage tests and TPD

The catalysts were initially exposed to 350 ppm NH_3 in the presence of 5% H_2O + 5% CO_2 for 1 h at 150 °C. After flushing with Ar + 5% H_2O for 30 min, the temperature was raised to 700 °C with a ramp speed of 10 °C min^{-1}. The outlet NH_3 concentration was monitored as a function of time and then converted to the cumulative NH_3 stored during the uptake period.

2.5.2. Reaction studies

The experiments of standard and rapid NH_3 SCR were conducted by increasing the reaction temperature stepwise while the reaction mixture was continuously fed during the whole temperature range (150–900 °C). The results for each temperature were obtained after the system had reached a steady-state and then the reactor temperature was increased to the next target reaction temperature. The experiments of 'standard' NH_3 SCR were performed with an inlet gas mixture consisting of 14% O_2, 5% CO_2, 350 ppm NH_3, 350 ppm NO, 5% H_2O and a balance of Ar. The reaction studies of 'rapid' NH_3 SCR were performed with an inlet gas mixture consisting of 14% O_2, 5% CO_2, 350 ppm NH_3, 175 ppm NO, 175 ppm NO_2, 5% H_2O and a balance of Ar. For comparison of the results, the reaction studies prior to and after thermal aging were performed in a predefined sequence of experiments. In the first stage, the activity measurements of 'standard'/'rapid' NH_3 SCR and NH_3 storage/TPD were conducted over the degreened catalysts. Then, the samples were subjected to different hydrothermal treatment steps, followed by activity measurements between each aging step.

3 Results and discussion

3.1. Chemical composition, textural, and structural characteristics of the Fe/SAPO-34 catalysts

3.1.1. ICP-AES, BET surface area and pore volume

The ICP-AES analysis of the Fe/SAPO-34 catalysts along with the pure SAPO-34 sample was carried out to quantify the amount of Fe, Al, Si, and P on the calcined powder samples. The results are listed in Table 1. The composition-dependent changes of the textural properties (S_{BET}, V_{pore}) of the samples are also summarized in Table 1. In addition, the N_2 adsorption–desorption isotherms for the different Fe/SAPO-34 catalysts are presented in Fig. 1.

In the case of Fe/SAPO-34 catalysts with different Fe loading, the ICP-AES analysis indicates that the synthesis with different concentrations of the Fe(III) nitrate nonahydrate precursor in the starting gel has resulted in SF catalysts with a final chemical composition, as follows: the SF-3 sample had the highest Fe loading (1.03 wt.%

Table 1
Chemical composition, specific surface area (S_{BET}) and total pore volume (V_{pores}) of the synthesized pure SAPO-34 and Fe/SAPO-34 catalysts with different Fe content.

Samples	Chemical composition (%)				(Si + P)/Al ratio	S_{BET} ($m^2\ g^{-1}$)	V_p ($cm^3\ g^{-1}$)
	Fe	Si	Al	P			
SAPO-34	<0.07	6.50	20.0	31.79	1.014	608.9	0.320
SF-1	0.27	6.73	20.2	14.5	1.051	606.4	0.328
SF-2	0.47	6.87	20.8	15.1	1.056	606.3	0.321
SF-3	1.03	5.61	12.9	12.3	1.388	671.3	0.365

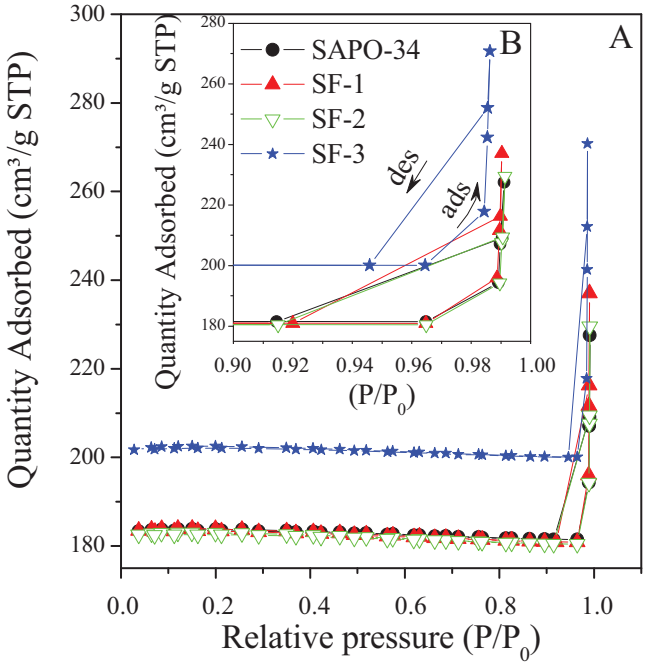

Fig. 1. N_2 adsorption–desorption isotherms of the synthesized SAPO-34 and the Fe/SAPO-34 catalysts with different Fe content. The inset (B) shows the hysteresis loop in the higher relative pressure (P/P_0) range of 0.9–1.0, similar to H3 type according to the IUPAC classification.

Fe), followed by SF-2 (0.47 wt.% Fe) and then SF-1 (0.27 wt.% Fe). The elemental analysis of the various samples also showed that the (Si + P)/Al ratios are all about 1.01–1.05 for the pure SAPO-34, SF-1 and SF-2 samples, which is similar to that reported in the literature for SAPO-34 [40]. Only in the case of the SF-3 catalyst with the highest Fe content, the (Si + P)/Al = 1.388 ratio is much higher. This higher (Si + P)/Al ratio of the SF-3 sample indicates that incorporation of large amount of Fe into the structure decreases the Al content significantly. Indeed, the iron content between SF-2 and SF-3 only increased with 0.57 wt.%, while the Al content decreased with as much as 7.9 wt.%. It should be noted that also Si and P has decreased in SF-3, but that Al decreased significantly more. Moreover, according to other studies in the literature, a ratio of (Si + P)/Al > 1 is an indication that the Si incorporation into the $AlPO_4$ framework occurs simultaneously through two substitution mechanisms [40,41]. One is a mechanism with one isolated Si atom substituting for P [41,42]. The other is a mechanism with double substitution of neighboring Al and P by two Si atoms [43]. Although all three Fe containing SAPO-34 samples and pure SAPO-34 in our study were prepared starting from a gel with identical Al:P:Si: morpholine molar ratios, the chemical composition of the SF-3 catalyst implies that the coexistence of Fe^{3+} ions in higher concentrations in the starting gel has an effect on the Al incorporation into the framework. As a result, the Al content in the SF-3 sample is significantly lowered and thus the (Si + P)/Al ratio also differs from the other samples, respectively. This effect can be explained by considering the synthesis of the Fe/SAPO-34 catalysts, where the iron precursor was added to the AlPO solution in the step before the addition of the silicon source with the morpholine. Therefore, it is likely that iron partially replaces the Al during the structure formation of the Fe/SAPO-34 under these synthesis conditions. This is also consistent with other reports where it has been found that the incorporation of metal ions in the SAPO structure takes place by a partial substitution of Al^{3+} sites in the framework to form P(nAl, (4-n) Me) chemical environments [44–47].

Table 1 also presents the results regarding the textural characteristics of the SAPO-34 and Fe/SAPO-34 catalysts synthesized with different Fe content. The analysis shows that compared to the pure SAPO-34 material, the synthesis of the SF-1 and SF-2 samples, having different Fe content did not result in any significant changes in the corresponding BET surface area (S_{BET}) and total pore volume. These three samples are all characterized with a high surface area in the range of 609–606 m^2/g. They also revealed similar V_{pore} (~0.32 cm^3/g), indicating that the incorporation of Fe^{3+} ions in the SAPO framework proceeds without significant occlusion of the pores in the network of the zeolite matrices. On the other hand, a considerable difference in the textural characteristics of the SF-3 catalyst was observed (Table 1). The SF-3 sample with the highest Fe content exhibits significantly higher S_{BET} and V_{pore} compared to the other samples. These results are also illustrated by the data in Fig. 1, presenting the N_2 adsorption–desorption isotherms for the different samples. It can be seen that the quantity of adsorbed N_2 is larger for the SF-3 catalyst, while the amounts for the other samples remained similar (Fig. 1A). Despite of the minor changes in the shape, the isotherms of the as-synthesized SAPO-34 and all three Fe-containing systems are similar to I type and exhibit a distinctive hysteresis loop (the inset B of Fig. 1) in the higher relative pressure (P/P_0) range of 0.9–1.0, similar to H3 type according to the IUPAC classification [48].

3.1.2. XRD

The structural investigations by means of XRD, presented in Fig. 2 also show that the characteristic reflections of the synthesized pure SAPO-34 and Fe/SAPO-34 samples very nearly coincide with those of the reference, commercial SAPO-34 product. This confirms that the Fe/SAPO-34 catalyst is characterized by the typical CHA structure for SAPO-34 reported in the literature [27]. The high intensity and the absence of any baseline drift indicate the high crystallinity of the samples without/or with only minor impurities. In addition, no diffraction peaks related to the presence of Fe oxide species were observed, which indicates that the Fe content is either below the instrumental detection limit or that Fe exists mostly incorporated as isolated ions or well dispersed small crystal iron oxide particles in the SAPO structure.

It is also possible to observe in Fig. 2 that compared with the parent SAPO-34, the intensities of the main diffraction peak (1 0 0) of the SF samples gradually diminish with increasing the Fe content, indicating that the modification affected the crystallinity of the SAPO-34 material. This can be very clearly seen especially in the XRD pattern of the SF-3 catalyst with the highest Fe loading where the intensity of the reflection (1 0 0) with maximum at about 18.99–19.1° is much lower than those of the other samples.

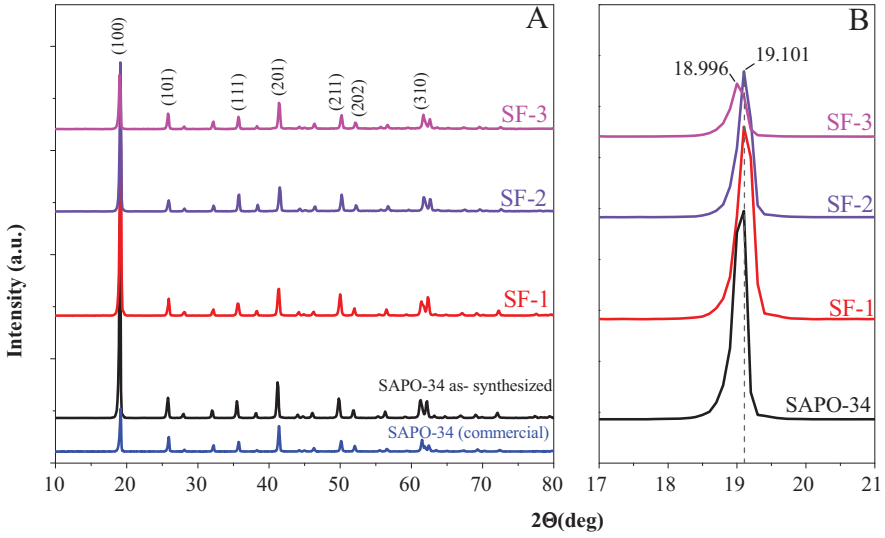

Fig. 2. XRD patterns of the synthesized SAPO-34 and the Fe/SAPO-34 catalysts with different Fe content, as well as the reference, commercial SAPO-34. The inset (B) shows the changes in the intensity of the main diffraction peak (1 0 0) in the XRD profiles of the samples, caused by the integration of Fe into the zeolite SAPO-34 framework.

Moreover, by more careful analysis of the XRD patterns, given in the Fig. 2B, a slight shift and broadening of the main diffraction peak (1 0 0) is apparent in the case of the SF-3 catalyst with an increased Fe content. To estimate qualitatively the lattice contraction/expansion of the SAPO-34 structure with the incorporation of higher amounts of Fe, the main reflection line (1 0 0) was used to determine the layer d_{100} spacing in the crystal lattice. The results show that the presence of higher content of Fe results in an increase of the d_{100} spacing from 5.391 Å ($2\theta = 19.10^\circ$) for SAPO-34 to 5.421 Å ($2\theta = 18.99^\circ$) for the SF-3 catalyst. This behavior was previously explained by a unit cell size expansion and decrease in crystallinity as a result of integration of Fe into the zeolite framework and proves that iron is incorporated into the SAPO-34 zeolite framework [49]. This is also consistent with other studies reported in the literature where it was found that the incorporation of transition metal ions into the SAPO-34 structure may provoke small changes in the crystallinity due to the differences in the sizes of the Al^{3+} ions (0.53 Å) substituted with Fe^{3+} ions (0.63 Å) in the SAPO-34 framework [35,50].

3.2. Flow reactor measurements

Further insight regarding the influence of Fe component was obtained by flow reactor measurements on the monolith washcoated Fe/SAPO-34 samples with different Fe content. The results in the next two sections are discussed with respect to the NH_3 storage and the NH_3 SCR performance of the Fe/SAPO-34 catalysts as a function of Fe content. Besides, the thermal stability after thermal aging of the Fe/SAPO-34 catalysts was also investigated.

3.2.1. NH3 storage tests and TPD

In Fig. 3A–C, time-dependent NH_3 uptake (at 150 °C) and TPD (150–700 °C) measurements over the fresh and hydrothermally treated Fe/SAPO-34 catalysts is presented. To test the thermal stability, a high temperature aging at 800 °C for 24 h in the presence of 5% H_2O, 14% O_2, 5% CO_2 was performed over the fresh SF catalysts. The inset (D) of Fig. 3 presents the amounts of NH_3 stored on the surface in mmol per gram catalysts as function of the Fe loading for both fresh and aged samples. It is visible in Fig. 3A–C that upon NH_3 admission at 150 °C the uptake process is immediately initiated. The NH_3 breakthrough appeared with a steady increase in the exit NH_3 concentration over time, gradually approaching the inlet NH_3 concentration level of 350 ppm. The NH_3 adsorption experiments performed over the fresh SF-1 and SF-2 samples showed almost identical NH_3 concentration profiles. Calculation also showed (Fig. 3D) that the amounts of stored NH_3 are similar for both SF-1 and SF-2 samples and near 1.35–1.37 mmol/g_{cat}. On the other hand, the NH_3 signal during the exposure period is noticeably delayed for the fresh SF-3 sample in comparison to the other two catalysts with the lower Fe content. As a result, the corresponding NH_3 storage ability of the SF-3 sample is increased and is near 1.5 mmol/g_{cat}. The NH_3 desorption signals observed in the TPD profiles of all SF catalysts (Fig. 3A–C) reveal a major feature positioned at about 370 °C without any significant temperature shift in the desorption maxima. However, the evolution of NH_3 in the course of the desorption process follows a trend of increasing intensities of the NH_3 peaks with increasing Fe content. This can be very clearly seen especially for the fresh SF-3 catalyst, showing again that the NH_3 storage ability is more pronounced for this catalytic system.

Concerning the results obtained after hydrothermal treatment of the Fe/SAPO-34 catalysts, it was found that the NH_3 uptake behaviour is similar to that of the fresh non-aged samples with very small deviations in the NH_3 concentration profiles. Based on the data presented in Fig. 3D, it can be seen that the thermal aging has only a minor effect on the amounts of NH_3 stored on the surface for all three SF catalysts. The loss of NH_3 storage ability after ageing is merely about 7–8% lower than that of the fresh samples. It is suggested that the decrease in NH_3 adsorption after hydrothermal treatment of the Fe/zeolites (ZSM-5, Y, mordenite, beta, ferrierite) SCR catalysts is related to zeolite dealumination which leads to irreversible deactivation and collapse of the crystalline structure [51]. It is found that the hydrothermal aging modifies the acid properties of the zeolites [52,20]. However, in our case, the activity of all three SF catalysts to store NH_3 is shown to perform remarkably well even after being hydrothermally treated under extreme temperature conditions, proving the high hydrothermal stability of the SAPO-34 framework modified with Fe. Shwan et al. [52] observed a decrease of the number of isolated and dimeric Fe ions and an increase of smaller Fe_yO_x clusters after hydrothermal treatment of an Fe/BEA catalyst. Such migration of the Fe ions can explain the loss in NH_3 storage capacity observed in the present experiments.

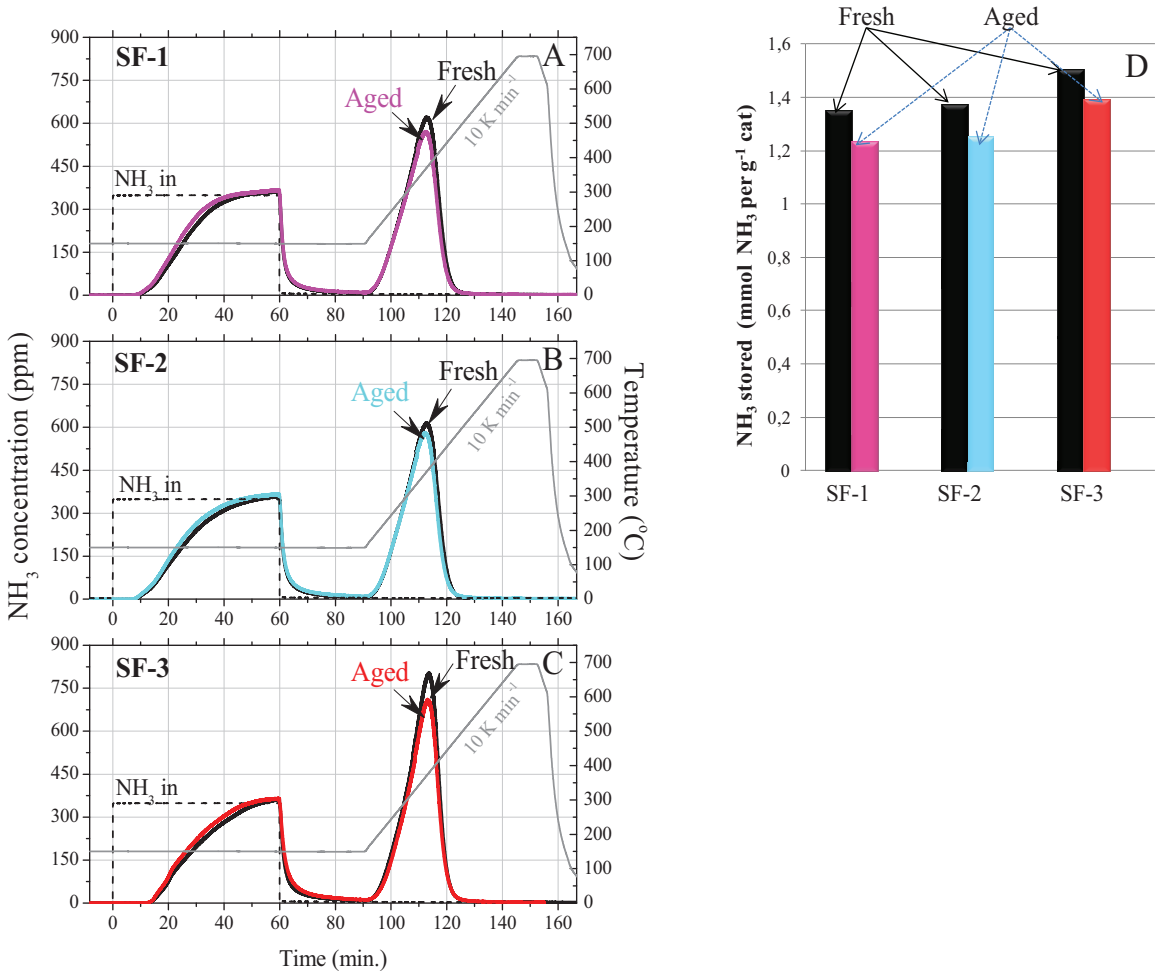

Fig. 3. Time-dependent NH_3 uptake (at 150 °C) and TPD (150–700 °C) analysis over the fresh and hydrothermally treated Fe/SAPO-34 catalysts with different Fe content (A–C). The hydrothermal aging was performed at 800 °C for 24 h in the presence of 5% H_2O, 14% O_2, 5% CO_2. The inset (D) presents the estimated amounts of NH_3 stored on the surface (mmol) per gram catalysts as function of the Fe loading for both fresh and aged samples.

3.2.2. Standard NH_3 SCR

The NO_x and NH_3 conversion as a function of the temperature (150–800 °C) of the reaction of standard NH_3 SCR for the different fresh and hydrothermally treated Fe/SAPO-34 catalysts are shown in Fig. 4A and B, respectively. The results in Fig. 4 show that the SCR activity of all catalysts is very limited by the reaction temperature in the range of 150–200 °C. A further increase in the reaction temperature to 250–350 °C (Fig. 4) gradually increases the activity of the SF catalysts for NO_x reduction, and a maximum NO_x conversion is achieved for all samples at 350 °C. Moreover, the NO_x reduction efficiency of the fresh, non-aged SF catalysts is found to increase with increasing Fe loading in the Fe/SAPO-34 catalysts. It can be seen in Fig. 4A that the fresh SF-3 catalyst (highest Fe content) reaches a maximum at 350 °C of about 91% NO_x conversion, while the SF-2 and SF-1 fresh catalysts exhibited a maximum of about 80% and 70% NO_x conversion, respectively.

In similar way, the experiments in the higher temperature region within 350–700 °C (Fig. 4) revealed that the fresh SF-3 catalyst is characterized with a maximum NO_x reduction (~90%) maintained constant over a broader temperature range (350–500 °C) than the other two fresh SF catalysts with lower Fe content. As observed in Fig. 4A for SF-2 and SF-1, after reaching a maximum at 350 °C, the NO_x reduction activity starts immediately to decline with further increasing the temperature. This can be clearly seen especially for the SF-1 catalyst, where the NO_x conversion attenuates more rapidly to the end of the experiments at 700 °C. Based on this, the activity to reduce NO_x of the fresh SF catalysts in the studied temperature range of 250–700 °C can be ranked in the following increasing order: SF-1 (fresh) < SF-2 (fresh) < SF-3 (fresh). Such behavior suggests that the incorporation of higher amounts of Fe in the SAPO framework has more significant effect to enhance the NO_x reduction performance of the fresh (degreened) catalysts. It should also be mentioned that the conversion of NH_3 for all catalysts is higher than the NO_x conversion. This is consistent with the results reported in other studies over Fe/zeolites where an overconsumption of NH_3 during NH_3 SCR was observed, which at low temperature is due to parasitic ammonia oxidation [53,54,55] and at high temperature due to regular ammonia oxidation.

In contrast to the fresh catalytic systems, the results in Fig. 4A for the SF samples after hydrothermal aging show that the presence of higher amounts of Fe substituted in the SAPO-34 framework has a negative effect on the thermal durability, which is profoundly lower in comparison to the catalyst with the lower Fe content. It can be seen that the hydrothermally treated SF-3 catalyst (Fig. 4A) is characterized by NO_x conversion profile similar to that of the fresh sample in the lower temperature region within 250–550 °C. However, the NO_x reduction activity of the aged SF-3 catalyst drops sharply at higher temperatures (550–800 °C), approaching a minimum in the NO_x conversion of about 20% at 800 °C.

The mechanisms of deactivation caused by hydrothermal aging of Fe/zeolites for NH_3 SCR have been thoroughly discussed by several research groups [20,52,56,57]. Accordingly, it was found

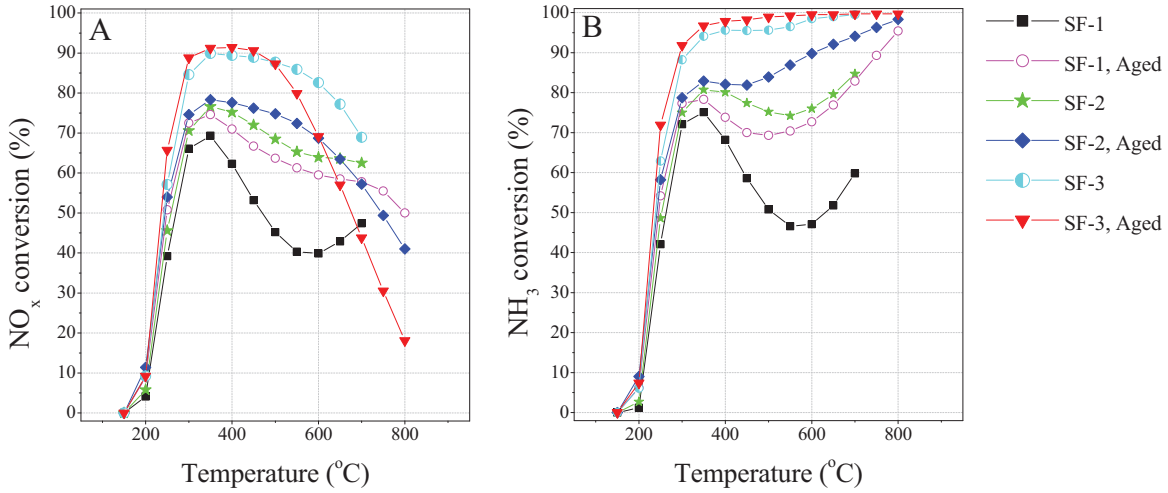

Fig. 4. NO_x (A) and NH_3 (B) conversion during standard NH_3–SCR as a function of the temperature of the reaction (150–800 °C) for the different fresh and aged Fe/SAPO-34 catalysts with different Fe content. The hydrothermal aging was performed at 800 °C for 24 h in the presence of 5% H_2O, 14% O_2, 5% CO_2. The reaction studies were performed in the presence of 350 ppm NO, 350 ppm NH_3, 14% O_2, 5% H_2O and 5% CO_2. The total gas flow was held constant at 3500 ml min^{-1}.

that Fe/ZSM-5 is characterized with deceased SCR activity after hydrothermal treatment above 500 °C. Among the different processes during hydrothermal aging, the deactivation of Fe/zeolite was found [20] to occur mainly by three parallel mechanisms, including a rapid dealumination, collapse of the zeolite structure, and migration and clustering of the active Fe species, which leads to the formation of FeO_x clusters that increase in size with time [20]. In addition, it was found that the Fe migration is not strongly related to the process of dealumination and the stability with respect to the SCR activity depends more on the stability of the active Fe species in the zeolites structure than the stability of the framework itself [20]. Although the mechanism of hydrothermal aging of the Fe/SAPO-34 catalysts in our study may be different compared to the suggested mechanism in the literature for Fe/ZSM-5, it is possible that the low NO_x reduction activity and stability of the aged SF-3 and SF-2 catalysts in the higher temperature region is related to similar changes of the active iron sites as described above. The minimal loss of NH_3 storage ability of both samples after aging is an indication that the hydrothermal treatment did not result in any significant damage of the zeolite structure. Moreover, the aged SF-3 and SF-2 catalyst preserve a high NO_x reduction conversion similar (and even higher for the aged SF-2) to that of the fresh samples at temperatures ≤550 °C. In agreement with other studies, it has been shown that the concentration of active Fe species is critical for the activity [20,57]. Indeed, the lower crystallinity observed, especially for the SF-3 catalyst was attributed to the unit cell size expansion provoked by integration of higher amounts of Fe into the zeolite SAPO-34 structure. This probably makes the Fe species incorporated in the SAPO-34 framework of the SF-3 catalysts unstable during hydrothermal aging. Thus, the higher mobility of Fe implies an easier Fe migration and formation of species that have limited NO_x reduction performance at high reaction temperatures. This suggestion is also consistent with other studies in the literature, where the migration of Fe is favored by the presence of water, which enhances the mobility of the cations in the zeolites structure [58,59]. Thus, metal-oxide clusters and particles with reduced activity are formed upon Fe migration [59,60].

In contrast to the aged SF-3, the results in Fig. 4A corresponding to the aged SF-1 catalyst with the lowest Fe content show an exclusive positive effect of the hydrothermal treatment on the NO_x reduction performance. Interestingly, an improved NO_x conversion of the aged compared to the fresh SF-1 sample is observed in the whole studied temperature range between 200 and 800 °C. This is accompanied by a consumption of significantly higher amounts of NH_3 (Fig. 4B) when increasing the temperature. The relatively high NO_x conversion (~60%) achieved for the aged SF-1 catalyst at 500 °C only slightly decreases until the end of the reaction at 800 °C. This low loss of NO_x reduction activity (of approximately, 15%) with increasing reaction temperature is an indication for the higher hydrothermal stability of the aged SF-1 compared to SF-3. Further, also SF-2 catalyst exhibit higher NO_x activity after aging in the temperature interval 200–650 °C.

In several studies, which focused on the effect of hydrothermal aging of Fe/ZSM-5, it was found that the NH_3 SCR performance is related to the nature of the active Fe species and their distributions on the catalysts [60–64]. In general, it is shown that the Fe species co-exist on the Fe/ZSM-5 surface mostly in the form of isolated Fe^{3+}, oligomeric Fe_xO_y clusters and Fe_2O_3 particles which distribution strongly depends on the Fe content [60–64]. Thus, different Fe species show different catalytic performance. One of the recent studies revealed that a high SCR activity of the Fe/ZSM-5 catalysts can be obtained by optimizing the Fe loading and maximizing the amount of isolated Fe^{3+} species by hydrothermal treatment of the catalysts [23]. This effect was explained by a partial migration and distribution of the Fe species which increases the relative concentration of the isolated Fe^{3+} sites. In another work, steam treatment at 600 °C for 5 h was reported to significantly improve the structure and activity of the Fe containing ALPO-5 for N_2O decomposition [49]. The beneficial effect of this procedure was explained by partial reduction of Fe^{3+} to Fe^{2+} and migration of the Fe ions to extra-framework positions upon steaming. Further, in a study by Nedyalkova et al. [65] an improved NO_x conversion were observed after treatment of the Fe/BEA catalyst at 700 °C in reducing conditions. Shwan et al. [66], explained this by the formation of isolated iron species during the high temperature reduction, based on DRIFT spectroscopy. In the light of these findings, it can be suggested that the observed increase in activity for SF-1 and SF-2 after hydrothermal aging can be related to similar Fe migration and formation of more stable Fe sites active in NH_3 SCR.

The NO_2 production during SCR was examined and the resulting NO_2 concentrations are shown in Fig. 5. The NO_2 concentrations were very low and in addition the N_2O (not shown) is negligible. Even though the NO_2 concentrations are low, clear trends are visible. The higher the Fe loading, the higher the NO_2 production is. This is consistent with results for Cu/BEA [8], where it was observed that higher exchange level resulted in copper sites that were more active for NO oxidation. It should be noted that during SCR conditions it

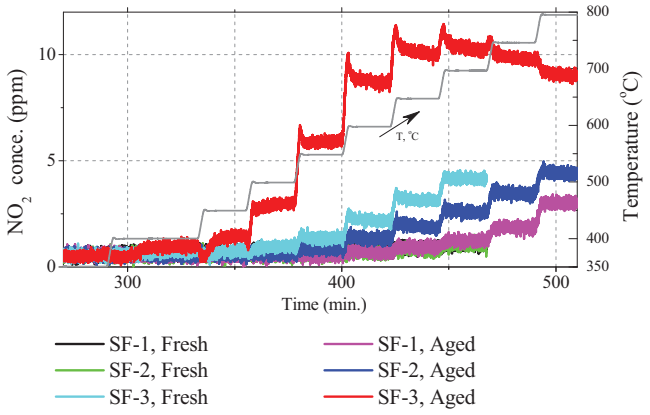

Fig. 5. Evolution of the product distribution of NO_2 in the outlet stream as a function of time during standard NH_3–SCR in the temperature range of 350–800 °C over the fresh and hydrothermally treated Fe/SAPO-34 catalysts with different Fe content.

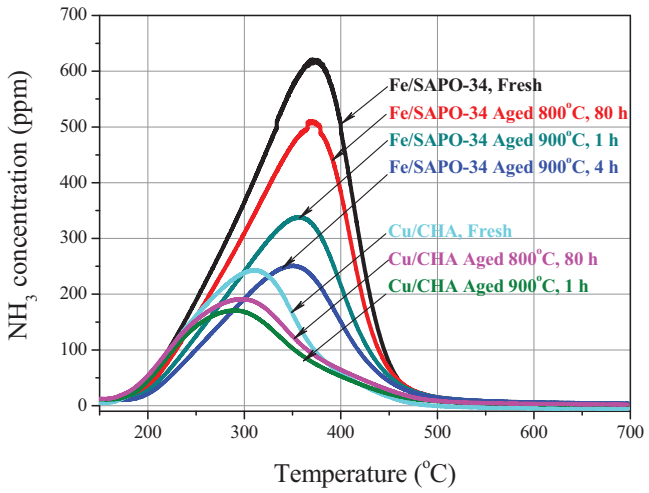

Fig. 6. NH_3-TPD (150–700 °C) analysis over the fresh and hydrothermally treated Fe/SAPO-34 (SF-1), as well as the reference, commercial fresh and aged Cu/CHA monolith samples.

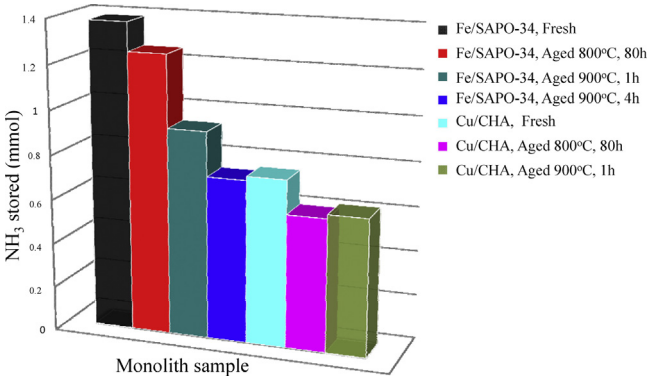

Fig. 7. Amounts of NH_3 stored on the surface (mmol) for the fresh and hydrothermally treated Fe/SAPO-34 catalyst (0.27 wt.% Fe), as well as a commercial Cu/CHA monolith sample as reference. Multiple long-term and accelerated aging protocols were carried out in the presence of 5% H_2O, 14% O_2, 5% CO_2, by varying the thermal treatment temperatures (800–900 °C) and times (1–80 h) of aging.

is possible that the ammonia inhibits the NO oxidation or possibly that NO oxidation occurs to a larger extent, but that the formed NO_2 reacts together with NH_3 and NO in the fast SCR mechanism. Another, interesting aspect is that the after hydrothermal aging the NO_2 formation is increased. These results are consistent with the observations by Shwan et al. [7], where it was seen that after mild aging the NO oxidation over Fe/BEA was increased.

3.2.3. *Hydrothermal stability of Fe/SAPO-34 compared to the commercially-available Cu/SAPO-34 SCR catalyst*

The data so far demonstrated that the SF-1 sample with the lowest Fe content has an interesting potential. The combination of relatively high NO_x reduction activity, especially in the higher temperature region within 550–800 °C, with the pronounced thermal durability makes this sample the most promising candidate for a high temperature NH_3 SCR applications. We therefore further studied the Fe/SAPO-34 catalyst with lowest Fe content (0.27% wt. Fe) in flow reactor measurements and comparing to the commercially-available Cu/CHA SCR system. To quantify the effect of the hydrothermal aging on Fe/SAPO-34 and Cu/CHA catalysts, multiple long-term and accelerated aging protocols were carried out by varying the thermal treatment temperatures (800–900 °C) and times (1–80 h) of aging in the presence of 5% H_2O, 14% O_2, and 5% CO_2.

3.2.3.1. NH3 storage tests and TPD. Ammonia storage is an important feature for transient operation and results from ammonia desorption during temperature programmed desorption (TPD) experiments using Fe/SAPO-34 and Cu/CHA, in both fresh and aged state, are shown in Fig. 6. In addition, Fig. 7 presents the amounts of NH_3 stored on the surface (mmol) for both fresh Fe/SAPO-34 and Cu/CHA monoliths as well as after aging. It is evident that the Fe/SAPO-34 sample exhibited significantly higher NH_3 storage compared to that of the commercial Cu/CHA catalyst. The washcoat loading of the commercial Cu/CHA catalyst is not known, however our Fe/SAPO-34 catalyst only contains about 101 g L^{-1} and commercial catalyst likely have significantly higher washcoat loading than our catalyst. The reason for that we use a low loading in our prepared catalysts is to decrease the risk of mass-transfer in the washcoat. Thus, the difference in ammonia storage per gram zeolite is likely even larger between our Fe/SAPO-34 and the commercial Cu/CHA. Another interesting feature for our Fe/SAPO-34 material is that the ammonia is more strongly bound to this zeolite compared to Cu/CHA, which is evident by the higher temperature for the desorption peak (see Fig. 6).

The study carried out over both aged Fe/SAPO-34 (SF-1) and Cu/CHA catalysts shows that the multiple hydrothermal treatment protocols carried out by increasing the temperature (800–900 °C) or time (1–80 h) of aging progressively impairs the effectiveness of the systems to store NH_3. However, even after aging at 900 °C for 1 h, the Fe/SAPO-34 catalyst still kept a higher NH_3 storage ability compared to the commercial Cu/CHA SCR system. These results clearly demonstrate the large stability at high aging temperatures (800–900 °C) of the synthesized Fe/SAPO-34 catalyst.

3.2.3.2. NO_x reduction in ('standard' and 'rapid') NH_3 SCR. Furthermore, activity measurements of the standard SCR reaction (NH_3/NO = 1) were conducted over the fresh and aged Fe/SAPO-34 (SF-1) and Cu/CHA catalysts. The Fe/SAPO-34 catalyst after aging gave very good NO_x reduction efficiency for high temperature NH_3 SCR applications (600–900 °C). This is clearly illustrated in Figs. 8 and 9, showing the NO_x and NH_3 conversions during standard NH_3 SCR (NH_3/NO ratio equal to 1) in the temperature range of 150–900 °C over both fresh and aged Fe/SAPO-34 and Cu/CHA catalysts, respectively.

The results in Fig. 8A and B corresponding to the Fe/SAPO-34 catalyst show a clear positive effect of the hydrothermal treatment of the sample at 800 °C for 80 h on the NO_x reduction performance in the whole studied temperature range between 200 and 800 °C.

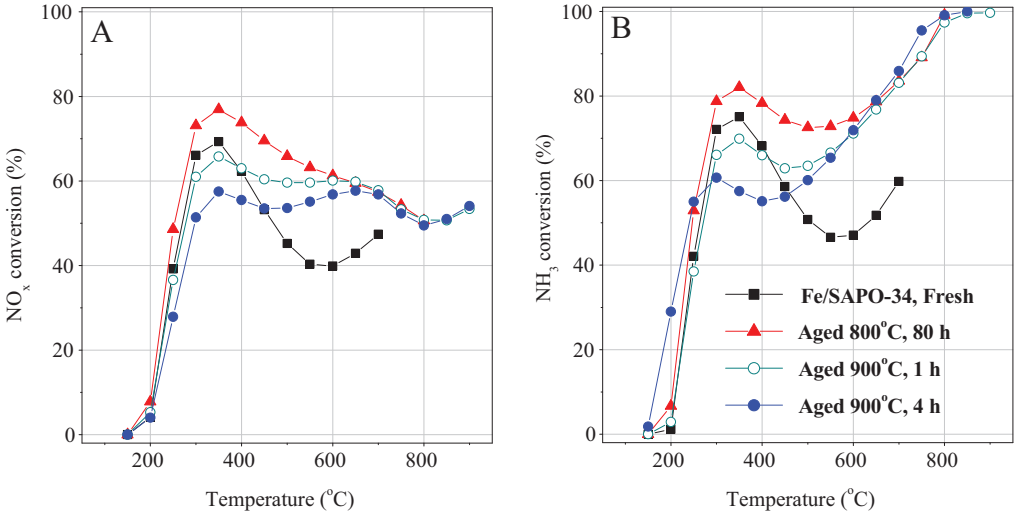

Fig. 8. NO_x (A) and NH_3 (B) conversions during standard NH_3 SCR ($NH_3/NO = 1$) as a function of the reaction temperature (150–900 °C) for the fresh and hydrothermally treated Fe/SAPO-34 (SF-1) catalyst. The inlet gas reaction mixture consisted of 14% O_2, 5% CO_2, 350 ppm NH_3, 350 ppm NO, 5% H_2O and a balance of Ar.

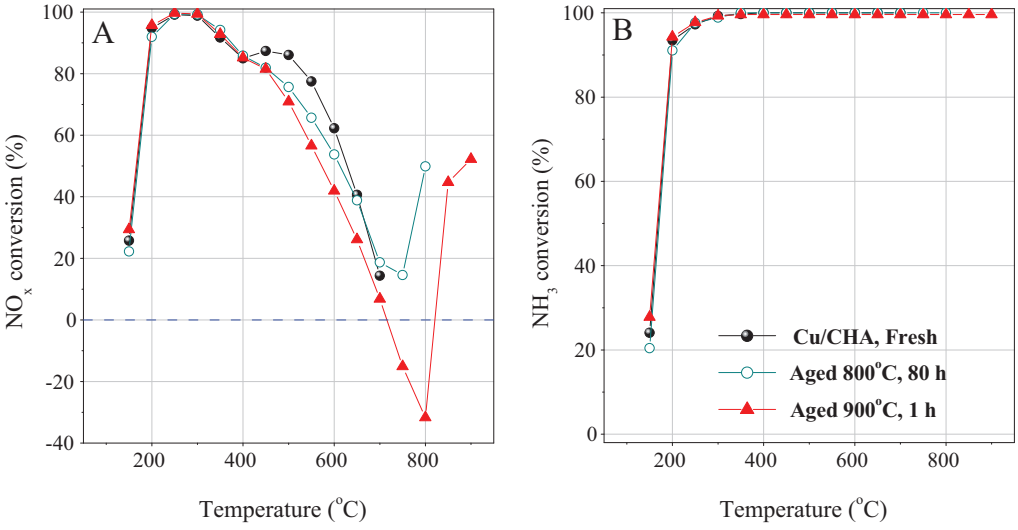

Fig. 9. NO_x (A) and NH_3 (B) conversions during standard NH_3 SCR ($NH_3/NO = 1$) as a function of the temperature of the reaction (150–900 °C) for the different fresh and hydrothermally treated commercial Cu/CHA catalysts. The inlet gas reaction mixture consisted of 14% O_2, 5% CO_2, 350 ppm NH_3, 350 ppm NO, 5% H_2O and a balance of Ar.

In particular, a significantly improved NO_x conversion is observed above 500 °C. It can be seen that the NO_x conversion increases up to ~60% at 500 °C after the exposure to such severe hydrothermal aging conditions and the activity decrease until 800 °C is quite small. It should also be mentioned that the conversion of NH_3 is higher (Fig. 8B) than the NO_x conversion which is consistent with the results reported in other studies over Fe/zeolites [54]. At low temperatures the overconsumption of NH_3 is due to the parasitic ammonia oxidation, as shown by Nedyalkova et al. [55] using isotopic labeled experiments, and at high temperatures due to the regular ammonia oxidation. One of the recent studies revealed that a high SCR activity of the Fe/ZSM-5 catalysts can be obtained by optimizing the Fe loading and maximizing the amount of isolated Fe^{3+} species by hydrothermal treatment of the catalysts [23]. This effect was explained by a partial migration and distribution of the Fe species, which increases the relative concentration of the isolated Fe^{3+} sites. In another work, steam treatment at 600 °C for 5 h was reported to have a significant improvement effect on the structure and activity of Fe containing ALPO-5 for N_2O decomposition [49]. The beneficial effect of this procedure was explained by partial reduction of Fe^{3+} to Fe^{2+} and migration of the Fe ions to extra-framework positions upon steaming by the formation of more stable active Fe sites. Further, Nedyalkova et al. [65] observed an activity increase for ammonia SCR after high temperature treatment of Fe/BEA in a reducing environment and the reason for this was suggested to be formation of isolated iron species during the high temperature reduction [66].

An additional increase in the aging temperature to 900 °C (Fig. 8A) progressively decreases the overall SCR performance of the Fe/SAPO-34 sample in the temperature region 250–600 °C. This is also evident with increasing the period of hydrothermal treatment of the catalyst, aged at 900 °C for 1 h and 4 h, respectively. However, the improved NO_x and NH_3 conversions (Fig. 8A and B) between 650 and 900 °C are preserved after aging at 900 °C and remain almost identical to the conversion achieved after the initial aging of the catalyst at 800 °C for 80 h. It can be seen that the Fe/SAPO-34 sample after the final hydrothermal treatment at 900 °C for 4 h is characterized with a maximum NO_x reduction conversion of about ~60% at 650 °C. The relatively high NO_x reduction activity of about 50–60% is maintained at all temperatures up to 900 °C.

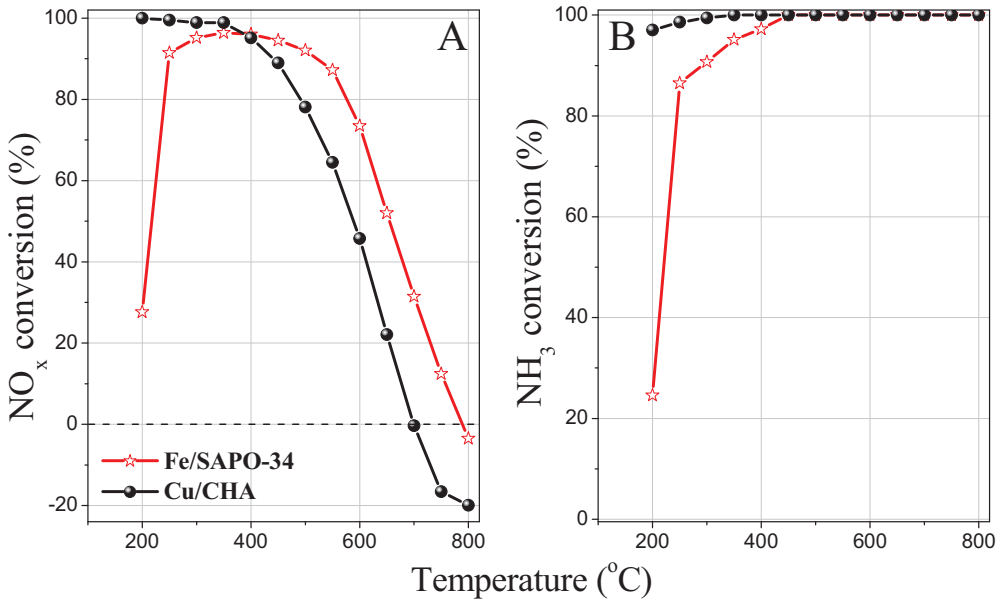

Fig. 10. NO_x (A) and NH_3 (B) conversion during rapid NH_3 SCR ($NH_3/NO_x = 1$, $NO_2/NO = 1$) as a function of the reaction temperature (150–800 °C) for the aged Fe/SAPO-34 (0.27 wt.% Fe) and the commercial Cu/CHA catalysts. The hydrothermal aging was performed at 800 °C for 80 h in the presence of 5% H_2O, 14% O_2, and 5% CO_2.

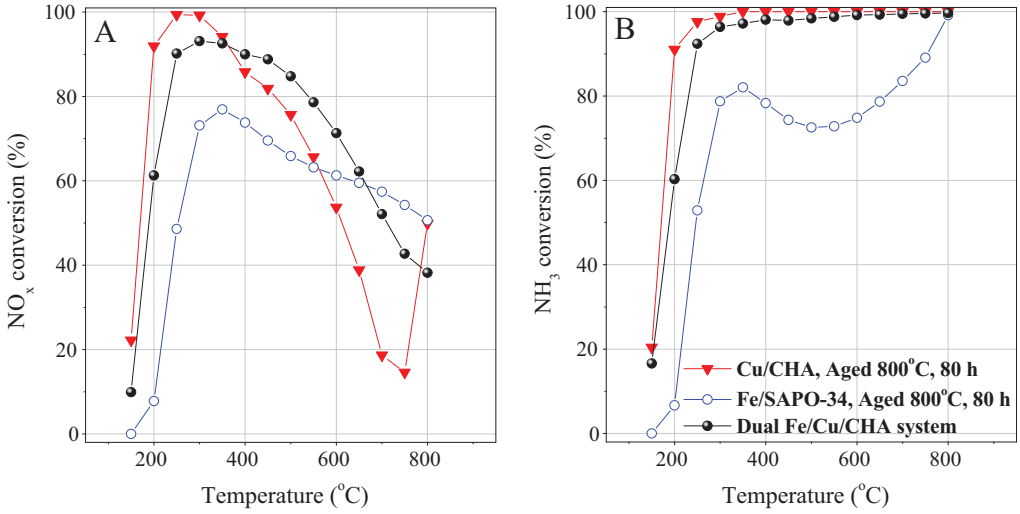

Fig. 11. NO_x (A) and NH_3 (B) conversions in the experiments of standard NH_3-SCR ($NH_3/NO = 1$) conducted in the range of 150–800 °C over the dual Fe/Cu/CHA system (2 cm total length, Fe/SAPO-34 (1 cm)/Cu/CHA (1 cm)) and over the single Fe/SAPO-34 and Cu/CHA monolith samples (2 cm length). For Fe/SAPO-34 the Fe loading was 0.27 wt.%. The activity measurements were conducted after hydrothermal aging of the monolith samples at 800 °C, 80 h in the presence of 5% H_2O, 14% O_2, 5% CO_2. The inlet gas reaction mixture consisting of 14% O_2, 5% CO_2, 350 ppm NH_3, 350 ppm NO, 5% H_2O and a balance of Ar.

In contrast to the Fe/SAPO-34 catalytic system, the analysis of the data in Fig. 9A after aging reveals that the Cu/CHA sample is relatively stable at low temperatures and the overall SCR performance in the region within 150–400 °C is barely affected by the hydrothermal treatment. However, more significant changes were observed at temperatures above 400 °C where the NO_x reduction performance is decreased after the aging procedures carried out at 800–900 °C. The most pronounced effect can be seen after aging at 900 °C for 1 h, where the NO_x reduction activity of the Cu/CHA drops notably, leading to negative NO_x conversion at 750–800 °C. In comparison the Fe/SAPO-34 system aged at 900 °C for 4 h achieved about 50% NO_x conversion in this range. On the contrary, the NH_3 conversion over the Cu/CHA (Fig. 9B) approaches almost total NH_3 conversion (100%) at temperatures above 300 °C. The negative NO_x conversion observed at temperatures up to 800 °C was explained previously in the literature [22] by the increased non-selective oxidation of NH_3 to NO_x during SCR over Cu/CHA. On the other hand, the drastic increase of the NO_x conversion observed in Fig. 9A at temperatures above 800 °C can be attributed to the direct decomposition of NO_x [67], leading to almost identical NO_x conversions over the Fe/SAPO-34 and the Cu/CHA at 900 °C.

The rapid SCR reaction was studied using a ratio of $NO_2/NO = 1$. For comparison of the results, the experiments were performed over the Fe/SAPO-34 and Cu/CHA catalysts both aged at 800 °C for 80 h. The NO_x and NH_3 conversion for the various reaction temperatures for both catalysts are presented in Fig. 10A and B. The presence of NO_2 in the feed increases the NO_x conversion over the Fe/SAPO-34 catalyst, at lower temperatures (250–500 °C), which exhibited significantly higher NO_x reduction activity compared to that during standard NH_3 SCR in the same range (Fig. 8). This is in agreement with other studies, showing the beneficial effect of the presence of NO_2 on the NO_x conversion on Fe/zeolites [68,69]. In addition, it is

visible that the Fe/SAPO-34 catalyst is more effective for NO_x abatement than the commercial Cu/CHA, at temperatures above 400 °C. It is worth mentioning that from 600 to 650 °C, for Fe/SAPO-34 and Cu/CHA, respectively, the NO_x conversion is negative due to ammonia oxidation to form NO. However, the Fe/SAPO-34 has lower values for the negative NO_x conversion compared to the commercial Cu/CHA. Thus at high temperatures the standard SCR reaction is preferred. Practically, the NO_2 is produced in a vehicle in the DOC and at these high temperatures only small amount of NO_2 will be produced in the DOC due to the thermodynamic equilibrium. Thus, it is very unlikely that the SCR catalyst will be exposed to 50% NO_2 at these high temperatures.

3.2.4. Combined system, including Fe/SAPO-34/Cu/SAPO-34 monoliths arrangement

For the standard SCR reaction (see Figs. 4 and 5) the commercial Cu/CHA catalyst possesses higher activity for NO_x below 550 °C, while the Fe/SAPO-34 sample is more active in the higher temperature region (≥600 °C). This is clearly illustrated in Fig. 11, comparing the results for both individual Fe/SAPO-34 and Cu/CHA catalysts aged at 800 °C for 80 h. Thus, it is of interest to investigate the possibility to achieve a high NO_x conversion over a wider temperature range by using both Fe/SAPO-34 and Cu/CHA catalysts simultaneously, which can combine the advantages of the individual samples. Therefore, activity measurements were conducted over a combined system, with Fe/SAPO-34 first, followed by the commercial Cu/CHA. Both samples were aged at 800 °C for 80 h and the results are presented in Fig. 11. The sequential configuration (2 cm total length) consists of a 1 cm long monolith of the synthesized Fe/SAPO-34 sample followed by a 1 cm long commercial Cu/CHA monolith. In addition, the results in Fig. 11A and B compare the NO_x and NH_3 conversion in the experiments conducted over the individual Cu/CHA and Fe/SAPO-34 monolith samples (2 cm length). At low temperatures (150–300 °C), the single Cu/CHA monolith sample exhibits slightly higher NO_x and NH_3 conversions compared to that of the dual Fe/SAPO-34-Cu/CHA arrangement. However, when increasing the reaction temperature to 350 °C, the NO_x and NH_3 conversion over the Fe/SAPO-34-Cu/CHA configuration almost approaches that of the single commercial Cu/CHA SCR system. The results in Fig. 11A clearly show that that the combination of Fe/SAPO-34 and Cu/CHA aged catalysts gives a significantly higher NO_x reduction performance in the temperature range of 400–750 °C compared to the effectiveness of both single systems. The dual arrangement of the catalysts achieved almost 55% NO_x conversion at 700 °C while the commercial single Cu/CHA SCR sample showed less than 20% conversion. Thus, we have demonstrated in this work that combining Fe/SAPO-34 with Cu/CHA results in a catalytic system with high activity for NH_3 SCR over a broad temperature range (200–800 °C).

4. Conclusions

The present work describes our investigation on the development of a novel Fe/SAPO-34 catalytic system for a high temperature NH_3 SCR application for NO_x reduction. In order to quantify deNO_x activity and hydrothermal stability, a series of Fe/SAPO-34 catalysts with different Fe content (0.27, 0.47, and 1.03 wt.% Fe) were prepared by Fe incorporation directly in the SAPO-34 synthesis. A combination of several characterization techniques was applied, such as ICP-AES, surface area measurements and XRD. In addition, to quantify the effect of the hydrothermal aging on the catalytic performance and thermal stability of the Fe/SAPO-34 catalyst, as well as a commercial Cu/CHA SCR catalyst, multiple long-term and accelerated aging protocols were carried out by varying the thermal treatment temperatures (800–900 °C) and times (1–80 h) of aging. Reaction studies over the fresh and hydrothermally aged samples during NH_3 -storage/temperature-programmed desorption (TPD), standard and rapid NH_3 SCR were performed as flow reactor experiments. Based on the results, the main conclusions are summarized as follows:

(a) The chemical composition, porous and crystalline structure of the parent SAPO-34 sample were found to be only slightly affected by addition of small amounts of Fe (0.27 wt.% Fe) in the framework zeolite structure. The Fe^{3+} ions directly added to the gel during synthesis of SAPO-34 may be incorporated by substituting the Al^{3+} ions in the framework of the material. More visible changes in the crystallinity were observed in the Fe/SAPO-34 catalysts with higher Fe content (1.03 wt.% Fe) which were attributed to the unit cell size expansion provoked by integration of higher amounts of Fe into the zeolite SAPO-34 framework.
(b) The Fe/SAPO-34 catalysts store large amounts of NH_3 even after being hydrothermally treated under extreme temperature conditions (at 800 °C for 80 h), demonstrating the hydrothermal stability of the modified Fe/SAPO-34 framework at high aging temperatures.
(c) Among the different Fe/SAPO-34 samples, the catalytic system with the lowest Fe content was shown to be the most efficient one regarding its NO_x reduction during NH_3 SCR and stability. The results show a high resistance of the Fe/SAPO-34 (0.27 wt.% Fe) catalyst toward deactivation under the oxidative atmosphere and a high hydrothermal stability of the system involved in a long-term aging.
(d) The Fe/SAPO-34 catalyst with the lowest Fe content (0.27 wt.% Fe) was found to be highly active for NO_x removal in a high temperature NH_3 SCR application (550–900 °C) and the activity was even increased after hydrothermal aging at 800 °C. It was shown that the synthesized Fe/SAPO-34 aged at 800 °C gives superior NO_x reduction efficiency for NH_3 SCR at high temperatures (600–750 °C) when compared to a commercial Cu/CHA SCR system.
(e) We have demonstrated in this work that combining Fe/SAPO-34 with Cu/CHA results in a catalytic system with high activity for NO_x reduction in NH_3 SCR over a broad temperature range (200–800 °C).

Acknowledgments

This work was performed in collaboration between Ford Motor Company and Chemical Engineering, Chalmers University. The funding from Swedish Foundation for Strategic Research (F06-0006) is gratefully acknowledged.

References

[1] H. Bosch, F. Janssen, Formation and control of nitrogen oxides, Catal. Today 2 (1988) 369–379.
[2] S. Brandenberger, O. Kröcher, A. Tissler, R. Althoff, The state of the art in selective catalytic reduction of NO_x by ammonia using metal-exchanged zeolite catalysts, Catal. Rev. Sci. Eng. 50 (2008) 492–531.
[3] N. Takahashi, H. Shinjoh, T. Iijima, T. Suzuki, K. Yamazaki, K. Yokota, H. Suzuki, N. Miyoshi, S.I. Matsumoto, T. Tanizawa, T. Tanaka, S.S. Tateishi, K. Kasahara, The new concept 3-way catalyst for automotive lean-burn engine: NO_x storage and reduction catalyst, Catal. Today 27 (1996) 63–69.
[4] L. Olsson, H. Sjövall, R.J. Blint, A kinetic model for ammonia selective catalytic reduction over Cu-ZSM-5, Appl. Catal. B Environ. 81 (2008) 203–217.
[5] C. Ciardelli, I. Nova, E. Tronconi, D. Chatterjee, B. Bandl-Konrad, M. Weibel, B. Krutzsch, Reactivity of NO/NO_2–NH_3 SCR system for diesel exhaust aftertreatment: identification of the reaction network as a function of temperature and NO_2 feed content, Appl. Catal. B Environ. 70 (2007) 80–90.
[6] I. Nova, C. Ciardelli, E. Tronconi, D. Chatterjee, B. Bandl-Konrad, NH_3–NO/NO_2 chemistry over V-based catalysts and its role in the mechanism of the Fast SCR reaction, Catal. Today 114 (2006) 3–12.

[7] S. Shwan, J. Jansson, J. Korsgren, L. Olsson, M. Skoglundh, Kinetic modeling of H-BEA and Fe-BEA as NH_3-SCR catalysts—effect of hydrothermal treatment, Catal. Today 197 (2012) 24–37.
[8] O. Mihai, C.R. Widyastuti, S. Andonova, K. Kamasamudram, J. Li, S. Joshi, N.W. Currier, A. Yezeretz, L. Olsson, The effect of Cu-loading on different reactions involved in NH_3-SCR over Cu-BEA catalysts, J. Catal. 311 (2014) 170–181.
[9] G.B.F. Seijger, P.K. Niekerk, K. Krishna, H.P.A. Calis, H. van Bekkum, C.M. van den Bleek, Screening of silver and cerium exchanged zeolite catalysts for the lean burn reduction of NO_x with propene, Appl. Catal. B Environ. 40 (2003) 31–42.
[10] J.H. Kwak, D. Tran, S.D. Burton, J. Szanyi, J.H. Lee, C.H.F. Peden, Effects of hydrothermal aging on NH_3-SCR reaction over Cu/zeolites, J. Catal. 287 (2012) 203–209.
[11] M. Wallin, C.-J. Karlsson, M. Skoglundh, A. Palmqvist, Selective catalytic reduction of NO_x with NH_3 over zeolite H–ZSM-5: influence of transient ammonia supply, J. Catal. 218 (2010) 354–364.
[12] J.H. Kwak, R.G. Tonkyn, D.H. Kim, J. Szanyi, C.H.F. Peden, Excellent activity and selectivity of Cu-SSZ-13 in the selective catalytic reduction of NO_x with NH_3, J. Catal. 275 (2010) 187–190.
[13] P.S. Metkar, M.P. Harold, V. Balakotaiah, Selective catalytic reduction of NO_x on combined Fe- and Cu-zeolite monolithic catalysts: sequential and dual layer configurations, Appl. Catal. B Environ. 111–112 (2012) 67–80.
[14] P.S. Metkar, M.P. Harold, V. Balakotaiah, Experimental and kinetic modeling study of NH_3-SCR of NO_x on Fe-ZSM-5, Cu-chabazite and combined Fe- and Cu-zeolite monolithic catalysts, Chem. Eng. Sci. 87 (2013) 51–66.
[15] P.S. Metkar, N. Salazar, R. Muncrief, V. Balakotaiah, M.P. Harold, Selective catalytic reduction of NO with NH_3 on iron zeolite monolithic catalysts: steady-state and transient kinetics, Appl. Catal. B Environ. 104 (2011) 110–126.
[16] R.Q. Long, R.T. Yang, Reaction mechanism of selective catalytic reduction of NO with NH_3 over Fe-ZSM-5 catalyst, J. Catal. 207 (2002) 224–231.
[17] S. Kieger, G. Delahay, B. Coq, B. Neveu, Selective catalytic reduction of nitric oxide by ammonia over Cu-FAU catalysts in oxygen-rich atmosphere, J. Catal. 183 (1999) 267–281.
[18] K.C.C. Kharas, H.J. Robota, D.J. Liu, Deactivation in Cu-ZSM-5 lean-burn catalysts, Appl. Catal. B Environ. 2 (1993) 225–237.
[19] S. Matsumoto, K. Yokota, H. Dio, M. Kimura, K. Sekizawa, S. Kasahara, Research on new $DeNO_x$ catalysts for automotive engines, Catal. Today 22 (1994) 127–146.
[20] S. Brandenberger, O. Kröcher, M. Casapu, A. Tissler, R. Althoff, Hydrothermal deactivation of Fe-ZSM-5 catalysts for the selective catalytic reduction of NO with NH_3, Appl. Catal. B Environ. 101 (2011) 649–659.
[21] J.H. Park, H.J. Park, J.J. Baik, I.S. Nam, C.-H. Shin, J.H. Lee, B.K. Cho, S.H. Oh, Hydrothermal stability of CuZSM5 catalyst in reducing NO by NH_3 for the urea selective catalytic reduction process, J. Catal. 240 (2006) 47–57.
[22] C.H.F. Peden, J.H. Kwak, S.D. Burton, R.G. Tonkyn, D.H. Kim, J.-H. Lee, H.-W. Jen, G. Cavataio, Y. Cheng, C.K. Lambert, Possible origin of improved high temperature performance of hydrothermally aged Cu/beta zeolite catalysts, Catal. Today 184 (2012) 245–251.
[23] X. Shi, F. Liu, W. Shan, H. He, Hydrothermal deactivation of Fe-ZSM-5 prepared by different methods for the selective catalytic reduction of NO_x with NH_3, Chin. J. Catal. 33 (2012) 454–464.
[24] C. Lambert, G. Cavataio, Development of the 2010 Ford Diesel Truck Catalyst System, in: I. Nova, E. Tronconi (Eds.), Urea-SCR Technology for $deNO_x$ After Treatment of Diesel Exhausts, Fundamental and Applied Catalysis, Springer, 2014, http://dx.doi.org/10.1007/978-1-4899-8071-7_21
[25] D.W. Fickel, E. D'Addio, J.A. Lauterbach, R.F. Lobo, The ammonia selective catalytic reduction activity of copper-exchanged small-pore zeolites, Appl. Catal. B Environ. 102 (2011) 441–448.
[26] Y. Watanabe, A. Koiwai, H. Takeuchi, S.-A. Hyodo, S. Noda, Multinuclear NMR. Studies on the thermal stability of SAPO-34, J. Catal. 143 (1993) 430–436.
[27] B.M. Lok, C.A. Messina, R.L. Patton, R.T. Gajek, T.R. Cannan, E.M. Flanigen, Silicoaluminophosphate molecular sieves: another new class of microporous crystalline inorganic solids, J. Am. Chem. Soc. 106 (1984) 6092–6093.
[28] M. Castro, S.J. Warrender, P.A. Wright, D.C. Apperley, Y. Belmabkhout, G. Pringruber, H.K. Min, M.B. Park, B.S. Hong, Silicoaluminophosphate molecular sieves STA-7 and STA-14 and their structure-dependent catalytic performance in the conversion of methanol to olefins, J. Phys. Chem. C 113 (2009) 15731–15741.
[29] Y. Zuo, L. Han, W. Bao, L. Chang, J. Wang, Effect of CuSAPO-34 catalyst preparation method on NO_x removal from diesel vehicle exhausts, Chin. J. Catal. 34 (2013) 1112–1122.
[30] U. Deka, I. Lezcano-Gonzalez, S.J. Warrender, A.L. Picone, P.A. Wright, B.M. Weckhuysen, A.M. Beale, Changing active sites in Cu–CHA catalysts: $deNO_x$ selectivity as a function of the preparation method, Microporous Mesoporous Mater. 166 (2013) 144–152.
[31] R.Q. Long, R.T. Yang, Superior Fe-ZSM-5catalyst for selective catalytic reduction of nitric oxide by ammonia, J. Am. Chem. Soc. 121 (1999) 5595–5596.
[32] R.Q. Long, R.T. Yang, Selective catalytic reduction of NO with ammonia over Fe^{3+}-exchanged mordenite (Fe–MOR): catalytic performance, characterization, and mechanistic study, J. Catal. 207 (2002) 274–285.
[33] J. Kielland, Individual activity coefficients of ions in aqueous solutions, J. Am. Chem. Soc. 59 (1937) 1675–1678.
[34] Y. Wei, D. Zhang, L. Xu, F. Chang, Y. He, S. Meng, B.-I. Su, Z. Liu, Synthesis, characterization and catalytic performance of metal-incorporated SAPO-34 for chloromethane transformation to light olefins, Catal. Today 131 (2008) 262–269.
[35] M. Kang, Methanol conversion on metal-incorporated SAPO-34s (MeAPSO-34s), J. Mol. Catal. A Chem. 160 (2000) 437–444.
[36] H.-X. Li, W.E. Cormier, B. Moden, Fe-SAPO-34 catalysts and methods of making and using the same. Patent application, Pub.No.:US2012/0251422A1, 2012, Pub. Date: Oct. 4.
[37] F. Gao, M. Kollár, R.K. Kukkadapu, N.M. Washton, Y. Wang, J. Szanyi, C.H.F. Peden, Fe/SSZ-13 as an NH_3-SCR catalyst: a reaction kinetics and FTIR/Mássbauer spectroscopic study, Appl. Catal. B Environ. 164 (2015) 407–419.
[38] S. Andonova, S. Tamm, L. Olsson, C.N. Montreuil, C.K. Lambert, Fe-SAPO-34 catalyst for use in NO_x reduction and method of making. Provisional patent application, Application Serial Number: 61/941,717, Filing date: February 19, 2014, Country: United States of America.
[39] A.M. Prakash, S. Unnikrishnan, Synthesis of SAPO-34: high silicon incorporation in the presence of morpholine as template, J. Chem. Soc. Faraday Trans. 90 (1994) 2291–2296.
[40] P. Wang, A. Lv, J. Hu, J. Xu, G. Lu, The synthesis of SAPO-34 with mixed template and its catalytic performance for methanol to olefins reaction, Microporous Mesoporous Mater. 152 (2012) 178–184.
[41] Y.X. Wei, D.Z. Zhang, Y.L. He, L. Xu, Y. Yang, B.L. Su, Z.M. Liu, Catalytic performance of chloromethane transformation for light olefins production over SAPO-34 with different Si content, Catal. Lett. 114 (2007) 30–35.
[42] R. Vomscheid, M. Briend, M.J. Peltre, P.P. Man, D. Barthomeuf, The role of the template in directing the Si distribution in SAPO zeolites, J. Phys. Chem. 98 (1994) 9614–9618.
[43] A.M. Beale, M.G. O'Brien, M. Kasuni, A. Golobi, M. Sanchez–Sanchez, A.J.W. Lobo, D.W. Lewis, D.S. Wragg, S. Nitkitenko, W. Bras, B.M. Weckhuysen, Probing ZnAPO-34 self-assembly using simultaneous multiple in situ techniques, J. Phys. Chem. C 115 (2011) 6331–6340.
[44] L. Xu, Z. Liu, A. Du, Y. Wei, Z. Sun, Synthesis, characterization, and MTO performance of MeAPSO-34 molecular sieves, Stud. Surf. Sci. Catal. 147 (2004) 445–450.
[45] W.L. Shea, R.B. Borade, A. Clearfield, Synthesis and properties of MgAPO-5, J. Chem. Soc. Faraday Trans. 89 (1993) 3143–3149.
[46] J.J. Li, Y. Guo, G.D. Li, J.S. Chen, C.J. Li, Y.C. Zou, Investigation into the role of MgO in the synthesis of MAPO-11 large single crystals, Microporous Mesoporous Mater. 79 (2005) 79–84.
[47] F. Deng, Y. Yue, T.C. Xiao, Y.U. Du, C.H. Ye, L.D. An, H.L. Wang, Substitution of aluminum in aluminophosphate molecular sieve by magnesium: a combined NMR and XRD study, J. Phys. Chem. 99 (1995) 6029–6035.
[48] F. Rouquerol, J. Rouquerol, K. Sing, Adsorption by Powders and Porous Solids, Academic Press, San Diego, USA, 1999.
[49] W. Wei, J.A. Moulijn, G. Mul, Effect of steaming of iron containing AlPO-5 on the structure and activity in N_2O decomposition, Microporous Mesoporous Mater. 112 (2008) 193–201.
[50] D. Zhang, Y. Wei, L. Xu, F. Chang, Z. Liu, S. Meng, B.L. Su, Z. Liu, MgAPSO-34 molecular sieves with various Mg stoichiometries: synthesis, characterization and catalytic behavior in the direct transformation of chloromethane into light olefins, Microporous Mesoporous Mater. 116 (2008) 684–692.
[51] K. Rahkamaa-Tolonen, T. Maunula, M. Lomma, M. Huuhtanen, R.L. Keiski, The effect of NO_2 on the activity of fresh and aged zeolite catalysts in the NH_3-SCR reaction, Catal. Today 100 (2005) 217–222.
[52] S. Shwan, J. Jansson, J. Korsgren, L. Olsson, M. Skoglundh, Kinetic modeling of H-BEA and Fe-BEA as NH_3-SCR catalysts—effect of hydrothermal treatment, Catal. Today 197 (2012) 24–37.
[53] A. Schuler, M. Votsmeier, P. Kiwic, J. Gieshoff, W. Hautpmann, A. Drochner, H. Vogel, NH_3-SCR on Fe zeolite catalysts—from model setup to NH_3 dosing, Chem. Eng. J. 154 (2009) 333–340.
[54] S. Shwan, J. Jansson, L. Olsson, M. Skoglundh, Chemical deactivation of Fe-BEA as NH_3-SCR catalyst—effect of phosphorous, Appl. Catal. B Environ. 147 (2014) 111–123.
[55] R. Nedyalkova, K. Kamasamudram, N.W. Currier, J. Li, A. Yezerets, L. Ollson, Experimental evidence of the mechanism behind NH_3 overconsumption during SCR over Fe-zeolites, J. Catal. 29 (2013) 101–108.
[56] C.H. Bartholomew, Mechanisms of catalyst deactivation, Appl. Catal. A Gen. 212 (2001) 17–60.
[57] S. Brandenberger, O. Kröcher, A. Wokaun, A. Tissler, R. Althoff, The role of Brønsted acidity in the selective catalytic reduction of NO with ammonia over Fe-ZSM-5, J. Catal. 268 (2009) 297–306.
[58] J.Y. Yan, G.D. Lei, W.M.H. Sachtler, H.H. Kung, Deactivation of Cu/ZSM-5Catalysts for lean NO_x reduction: characterization of changes of Cu state and zeolite support, J. Catal. 161 (1996) 43–54.
[59] E.J.M. Hensen, Q. Zhu, M. Hendrix, A.R. Overweg, P.J. Kooyman, M.V. Sychev, R.A. van Santen, Effect of high-temperature treatment on Fe/ZSM-5 prepared by chemical vapor deposition of $FeCl_3$: I. Physicochemical characterization, J. Catal. 221 (2004) 560–574.
[60] O. Kröcher, M. Devadas, M. Elsener, A. Wokaun, N. Söger, M. Pfeifer, Y. Demel, L. Mussmann, Investigation of the selective catalytic reduction of NO by NH_3 on Fe-ZSM5 monolith catalysts, Appl. Catal. B Environ. 66 (2006) 208–216.
[61] M. Iwasaki, K. Yamazaki, K. Banbo, H. Shinjoh, Characterization of Fe/ZSM-5 $DeNO_x$ catalysts prepared by different methods: relationships between active Fe sites and NH_3-SCR performance, J. Catal. 260 (2008) 205–216.

[62] S. Brandenberger, O. Kröcher, A. Tissler, R. Althoff, The determination of the activities of different iron species in Fe-ZSM-5 for SCR of NO by NH_3, Appl. Catal. B Environ. 95 (2010) 348–357.
[63] M. Schwidder, K.M. Santhosh, K. Klementiev, M.M. Pohl, A. Brückner, W. Grünert, Selective reduction of NO with Fe-ZSM-5 catalysts of low Fe content: I. Relations between active site structure and catalytic performance, J. Catal. 231 (2005) 314–330.
[64] S. Brandenberger, O. Kröcher, A. Tissler, R. Althoff, Estimation of the fractions of different nuclear iron species in uniformly metal-exchanged Fe-ZSM-5 samples based on a Poisson distribution, Appl. Catal. A Gen. 373 (2010) 168–175.
[65] R. Nedyalkova, S. Shwan, M. Skoglundh, L. Olsson, Improved low-temperature SCR activity for Fe-BEA catalysts by H_2-pretreatment, Appl. Catal. B Environ. 138–139 (2013) 373–380.
[66] S. Shwan, J. Jansson, L. Olsson, M. Skoglundh, Effect of post-synthesis hydrogen-treatment on the nature of iron species in Fe-BEA as NH_3-SCR catalyst, Catal. Sci. Technol. 4 (2014) 2932.
[67] C. Tofan, D. Klvana, J. Kirchnerova, Decomposition of nitric oxide over perovskite oxide catalysts: effect of CO_2, H_2O and CH_4, Appl. Catal. B Environ. 36 (2002) 311–323.
[68] M. Colombo, I. Nova, E. Tronconi, A comparative study of the NH_3-SCR reactions over a Cu-zeolite and a Fe-zeolite catalyst, Catal. Today 151 (2010) 223–230.
[69] M. Devadas, O. Krocher, M. Elsener, A. Wokaun, N. Söger, M. Pfeifer, Y. Demel, L. Mussmann, Influence of NO_2 on the selective catalytic reduction of NO with ammonia over Fe-ZSM5, Appl. Catal. B Environ. 67 (2006) 187–196.